Collective behavior of globally coupled Langevin equations with colored noise in the presence of stochastic resonance

Bo Yang, Xiao Zhang, Lu Zhang, and Mao-Kang Luo*

Department of Mathematics, Sichuan University, 610065, Chengdu, Sichuan, China

(Received 28 November 2015; revised manuscript received 25 February 2016; published 12 August 2016)

The long-time collective behavior of globally coupled Langevin equations in a dichotomous fluctuating potential driven by a periodic source is investigated. By describing the collective behavior using the moments of the mean field and single-particle displacements, we study stochastic resonance and synchronization using the exact steady-state solutions and related stability criteria. Based on the simulation results and the criterion of the stationary regime, the notable differences between the stationary and nonstationary regimes are demonstrated. For the stationary regime, stochastic resonance with synchronization is discussed, and for the nonstationary regime, the volatility clustering phenomenon is observed.

DOI: 10.1103/PhysRevE.94.022119

I. INTRODUCTION

In recent decades, stochastic resonance (SR) has been studied widely [1–6]. In a broad sense, the main effect of SR is that an intermediate noise intensity can lead to the maximum response of a stochastic system [7,8].

For the environmental fluctuation of a stochastic system, while early investigations of SR considered additive white noise [9–14], more recent works have considered multiplicative colored noise [7,15–25]. While additive white noise can lead to SR in nonlinear systems, multiplicative colored noise can lead to SR even in linear systems. Furthermore, colored noise has been found in various systems, especially biological systems [26,27]. One of the most important colored noises is dichotomous noise [28,29]. Dichotomous noise is bounded noise, which is fairly realistic for physical, engineering, and biological systems [27,30,31]. In addition, dichotomous noise can be reduced to Gaussian white noise or white shot noise, which is of theoretical interest [28].

Most stochastic systems consist of coupled particles, which can be regarded as complex networks [32]. Following the development of complex networks, the investigations of SR have been extended to coupled stochastic systems [10–14]. In addition, the investigations into coupled stochastic systems have suggested that both the noise parameters and the coupling can affect the response of the system [13,14].

Recently, most SR investigations have studied the effects of multiplicative dichotomous noise in uncoupled systems [7,15–22], except for a few works that studied coupling cases [23–25]. These works show us that coupling can induce some interesting phenomena. For example, mean-field coupling can induce SR [23], and local additive coupling affects the output intensity of SR [24,25]. In Refs. [24,25], the collective behavior is described by the first moments of the response of the system. However, the need to study beyond the first moment was shown early in Refs. [33,34]. Based on this need, for an uncoupled particle, the effect of the second moment is studied in the stationary regime with the corresponding criteria [8,35]. Here, for clarity, the term stationary regime means that the first moment and the second moment (or variance) are both bounded [8,35]. Therefore, for coupled particles with dichotomous noise in the presence of SR, studying their collective behavior in the stationary regime is very interesting.

To analyze their collective behavior, we introduce globally coupled particles in a randomly switching potential driven by a periodic source. Applying the formulas of differentiation [29], we profile the collective behavior using the moments of the mean field and the single particle displacements, and then determine the related stability criteria. Using the analytic results and numerical simulation, we analyze the collective behavior of the coupled stochastic system. In the stationary regime, the first moment of the response of the system can be estimated reliably. We find that the SR phenomenon and the coupled particles perform synchronously as the same as the mean field. Increasing the coupling intensity or the number of particles can reduce the relaxation time for synchronization. For the nonstationary regime, the first moment of the response of the system cannot be estimated reliably due to the divergent variance, and the divergent variance can induce volatility clustering, which indicates a heavy-tailed distribution [36]. This potential mechanism shows a connection between SR and heavy-tailed distributions. Therefore, these results can provide some useful insights for the investigation of the fruitful noise-induced phenomena in stochastic systems.

The structure of the paper is as follows. In Sec. II, we introduce the model of the coupled Langevin equations and then determine the related explicit results. In Sec. III, we analyze the collective behavior of the coupled Langevin equations with the explicit results. In Sec. IV, some discussions conclude this paper.

II. COUPLED LANGEVIN SYSTEM

A. Model

Considering a system of N harmonically coupled particles driven by a periodic sine source in a fluctuating potential, we introduce the following coupled Langevin equations (in dimensionless form):

$$\frac{dx_i}{dt} + (a + \xi_t)x_i = \epsilon \sum_{n=1}^{N}(x_n - x_i) + A \sin \Omega t, \quad i = 1, \ldots, N, \tag{1}$$

*makaluo@scu.edu.cn

where $A \geqslant 0$ and $\Omega > 0$ are the external periodic driven strength and frequency, respectively, and $\epsilon \geqslant 0$ is the coupling coefficient. Fluctuation of the potential parameter $a > 0$ is described by a dichotomous Markov process [28,29], also called random telegraph noise, ξ_t, which randomly switches between two values $\pm\sigma$, $\sigma > 0$ with the mean value

$$\langle \xi_t \rangle = 0$$

and the autocorrelation

$$\langle \xi_t \xi_\tau \rangle = \sigma^2 \exp(-2v|t-\tau|),$$

where $(2v)^{-1}$ is the mean waiting time, $\langle \dots \rangle$ indicates averaging over all realizations of the noise.

The fluctuating potential randomly switches between

$$V_\pm(x) = (a \pm \sigma)\frac{x^2}{2}.$$

Note that (a) for $0 < \sigma < a$, both $V_+(x)$ and $V_-(x)$ are stable, and (b) for $0 < a < \sigma$, $V_+(x)$ is stable and $V_-(x)$ is not stable. For case (a), the system Eq. (1) is obviously stable. However, for case (b), because the potential switches between the stable state and the unstable state, the stability of the response of system Eq. (1) is not trivial. This kind of fluctuating potential barrier can be found in various systems, for example, an ATP-ADP potential. The ATP-ADP potential can be produced by the repeated binding-release cycle in a biological system [37–39]. This model Eq. (1) can be regarded as coupled protein motors in an ATP-ADP potential driven by a periodic source. In Ref. [25], research into this type of model Eq. (1) with locally coupled particles implies some potential applications in various scenarios [40–42].

B. Mean field

To analyze the collective behavior of the coupled Langevin Eq. (1), we introduce the mean field,

$$S = \frac{\sum_{i=1}^{N} x_i}{N},$$

and the corresponding fluctuation,

$$\tilde{S}^2 = (S - \langle S \rangle)^2.$$

The mean field S is a profile of the average displacement of all N particles and the fluctuation $\tilde{S}^2$ measures how far the particles of system Eq. (1) are spread out from the first moment of the mean field S.

By statistically averaging all N equations in system Eq. (1), with the mean field S, we obtain

$$\frac{dS}{dt} + (a + \xi_t)S = A \sin \Omega t. \tag{2}$$

To find the steady-state solution of the first moment, we apply the results in the Appendix. Then, we can write the steady-state solution of the first moment of Eq. (2) as

$$\langle S(t) \rangle_{\mathrm{E}} = A|H_{10}(\mathrm{j}\Omega)| \sin(\Omega t + \phi_1), \tag{3}$$

with the parameters given in Eqs. (A10) and (A11). The corresponding stability criteria are

$$\sigma^2 < a^2 + 2av \tag{4}$$

for the first moment, and

$$\sigma^2 < a^2 + av \tag{5}$$

for the variance.

Noticing that $a^2 + av < a^2 + 2av$, we obtain one of the main results in this paper: the stability criterion for both the first moment and the variance of the mean field is

$$\sigma^2 < \sigma_{\mathrm{M}}^2 = a^2 + av, \tag{6}$$

which we call *the stationary regime criterion* due to the following discussion in Sec. III A.

C. Single particle

To discuss the collective behavior of the coupled Langevin Eq. (1) in detail, we also need to analyze a single particle of system Eq. (1), say the ith, which is governed by the following equation:

$$\frac{dx_i}{dt} + (a + \xi_t)x_i = N\epsilon(S - x_i) + A \sin \Omega t.$$

Denoting the deviation of the ith particle's displacement from the mean field by

$$\Delta_i = x_i - S,$$

we can obtain

$$\frac{d\Delta_i}{dt} + (a + N\epsilon)\Delta_i + \xi_t \Delta_i = 0.$$

Averaging the above equation, we arrive at

$$\frac{d\langle \Delta_i \rangle}{dt} + (a + N\epsilon)\langle \Delta_i \rangle + \langle \xi_t \Delta_i \rangle = 0. \tag{7}$$

For convenience, in the following, the subscript i will be dropped.

Similarly, using the results in the Appendix, we can find the steady-state solution and the corresponding criteria just by the replacing rules that $a \mapsto a + N\epsilon$ and $A \mapsto 0$ for Eq. (A1). Then, using Eq. (7), the steady-state solution for the first moment is

$$\langle \Delta \rangle_{\mathrm{E}} = 0, \tag{8}$$

with the stability criterion

$$\sigma^2 < (a + N\epsilon)^2 + 2v(a + N\epsilon), \tag{9}$$

and the steady-state solution for the second moment is

$$\langle \Delta^2 \rangle_{\mathrm{E}} = 0, \tag{10}$$

with the stability criterion

$$\sigma^2 < (a + N\epsilon)^2 + v(a + N\epsilon). \tag{11}$$

Because i is arbitrary, we emphasize that the above results uniformly hold for any particle in system Eq. (1).

Based on criteria Eqs. (9) and (11), the stability criterion of the deviation of a single particle for both the first and the second moments is

$$\sigma^2 < \sigma_{\mathrm{S}}^2 = (a + N\epsilon)^2 + v(a + N\epsilon), \tag{12}$$

which is one of the main results of this paper. Based on the analysis in Sec. III B, we call it *the synchronization criterion*.

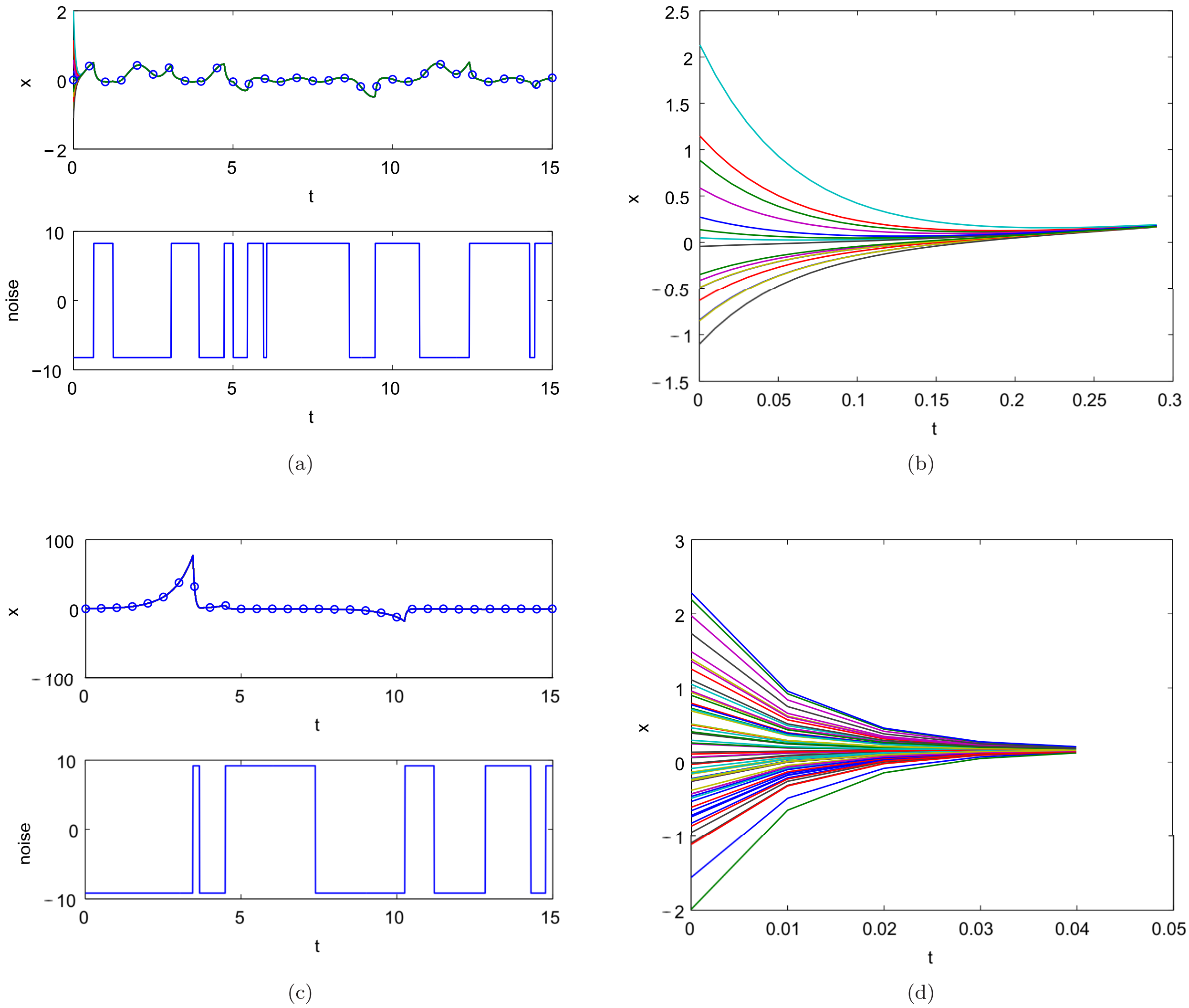

FIG. 1. The realization of system Eq. (1) and the corresponding noise realization with $a = 8$, $A = 1$, $\Omega = 1.5\pi$, $v = 1$, and $\epsilon = 1$ for different numbers of particles. Figures 1(a) and 1(b) are depicted with $N = 16$ and $\sigma^2 = a^2 + 0.5av$. Figures 1(c) and 1(d) are depicted with $N = 64$ and $\sigma^2 = a^2 + 1.5av$. In the top panels of Figs. 1(a) and 1(c), the colored solid lines depict the trajectories of the particles and the open circles depict the corresponding mean field. In the bottom panel of Figs. 1(a) and 1(c), the solid lines depict the corresponding noise realization of the top panels of Figs. 1(a) and 1(c), respectively. The realizations near the initial time ($t = 0$) in the top panels of Figs. 1(a) and 1(c) are shown in Figs. 1(b) and 1(d), respectively. Different colored lines indicate different particle displacements.

III. COLLECTIVE BEHAVIOR

In this section, we discuss the collective behavior of stochastic system Eq. (1) based on the above results and provide intuitive simulation results. For the simulations in this paper, we apply the numerical method proposed in Ref. [43].

A. Stationary regime

From criteria Eqs. (4) and (5) for the mean field, even the first moment is stable; however, the variance might be unstable. This behavior will lead to a nonstationary fluctuation around the average value, which will notably affect both practical application and numerical simulation. For illustration, the intuitive simulation results are given in Fig. 1.

In Figs. 1(a) and 1(c), although both noise intensities satisfy the stability criterion of the first moment Eq. (4), the fluctuation of the response in Fig. 1(a) is much smaller than in Fig 1(c). The remarkable difference in the fluctuation can be explained by the instability of the variance. Furthermore, the instability of the variance can lead to an unreliably estimated value [see Fig. 3(b)].

From the realizations in Fig. 2(a), we can intuitively observe the volatility clustering phenomenon, which indicates that large changes tend to be followed by large changes of either sign, and small changes tend to be followed by small changes [36]. Volatility clustering indicates the heavy-tailed distribution [36]. For a fixed time, the realizations of the mean field of system Eq. (1) show a power-law-like distribution with a heavy tail in Fig. 2.

B. Synchronization

From Eqs. (8) and (10), we can infer that all the realizations of the deviation are zero except for a set of measure zero. This implies that each particle of system Eq. (1) is almost

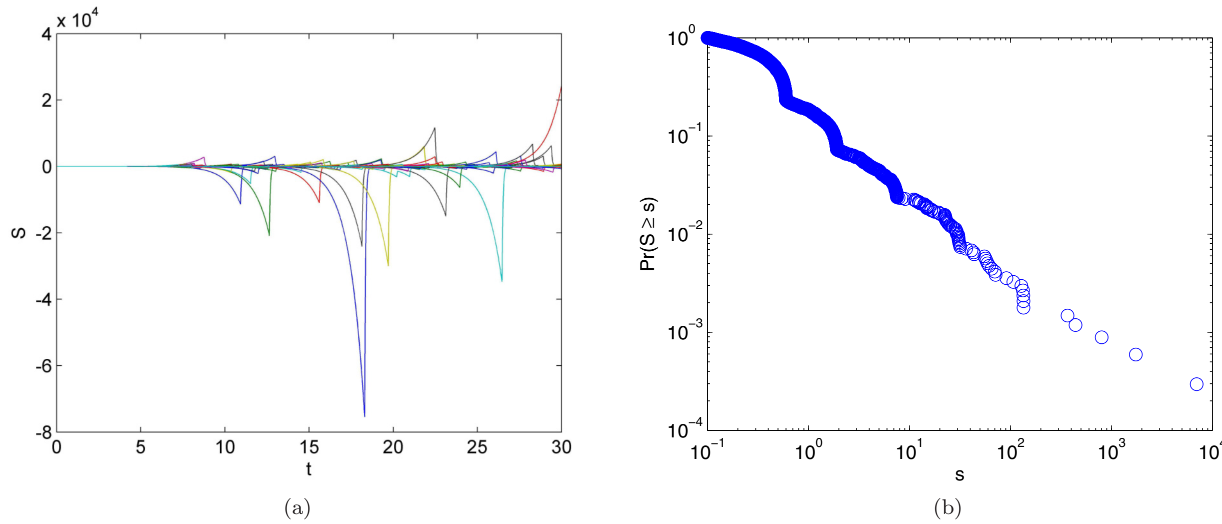

FIG. 2. The realization of the mean field in the nonstationary regime and the corresponding heavy-tailed distribution of the mean field. The parameters are $a = 8$, $A = 1$, $\Omega = 1.5\pi$, $\epsilon = 1$, $v = 1$, and $\sigma^2 = a^2 + 1.5av$. Figure 2(a) shows 10^4 realizations of the mean field. Figure 2(b) shows that the corresponding distribution of the realizations satisfied $S > 0.1$ at $t = 22$.

synchronized with the mean field S in the long-time regime (see Fig. 1).

From criteria Eqs. (6) and (12), we can infer that

$$\sigma_{\mathrm{M}} \leqslant \sigma_{\mathrm{S}}, \tag{13}$$

which means that particles with different initial conditions can move uniformly with the mean field in the stationary regime [see Fig. 1(a)]. For a large number of particles, N, the particles can show this synchronization even in the nonstationary regime [see Fig. 1(c)].

From the term $N\epsilon$ in criterion Eq. (12), the coupling intensity ϵ plays the same role as the number of particles, N. Thus, without loss of generality, we let the coupling intensity be one in the following analysis and simulation. As the number of particles increases, the relaxation time for synchronization decreases [see Figs. 1(b) and 1(d)], because the real parts of the eigenvalues are moving away from the origin in the negative direction as the number of particles increases. Here, we mention that the coupling only affects the relaxation time for synchronization, and the essential reason for the synchronization is the uniform influence of the randomly switching potential, which can be inferred from inequality

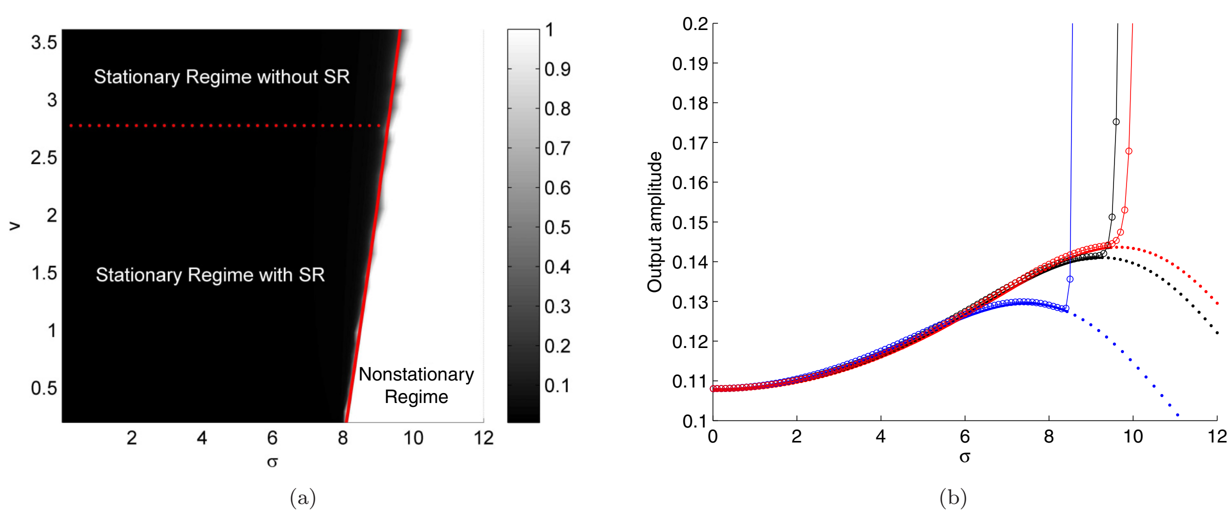

FIG. 3. A plot of the phase diagram in the v-σ plane and the output amplitude of the first moment of the mean field. The parameter region is plotted in Fig. 3(a) with $a = 8$, $A = 1$, $\Omega = 1.5\pi$. For the simulation result in Fig. 3(a), the value is defined by $Q = 1 - \exp(-\int_0^T \langle x^2\rangle dt/T)$, which takes a value from 0 (dark) to 1 (light). A lighter Q value indicates a larger $\int_0^T \langle x^2\rangle dt/T$, and $T = 300$ was used for the simulation with time step 0.003. For the analytical result in Fig. 3(a), the red solid line is the critical line between the stationary regime and the nonstationary regime, and the red dotted line is the critical line for the emergence of SR in the stationary regime. In Fig. 3(b), the output amplitude of the first moment is plotted for $v \approx 0.88 < \Omega^2/a$ (blue), $v = 2.73 \approx \Omega^2/a$ (black), and $v \approx 3.22 > \Omega^2/a$ (red); for the analytical results, the solid part means the output amplitude in the stationary regime, and the dotted part means the output amplitude in the nonstationary regime; the open circle lines stand for the corresponding numerically estimated results. All the estimated results are obtained from 10^4 realizations.

Eq. (13) by using a zero coupling intensity. As a result, in the stationary regime, we can analyze the behavior of all of the particles just by analyzing the mean field. Therefore, in the following discussion, we focus on the mean field.

C. Stochastic resonance

From Eq. (3), because the output amplitude of $\langle S\rangle_{\mathrm{E}}$ achieves its extreme value at $\sigma_0^2 = a^2 + 2av - \Omega^2$, we can find the criterion for the emergence of SR:

$$\max\left(\frac{\Omega^2 - a^2}{2a}, 0\right) < v < \frac{\Omega^2}{a}. \tag{14}$$

But if one needs a stationary response, the criterion for the stationary regime Eq. (6) should satisfy as well. Although the criteria Eqs. (6) and (14) have nothing to do with the coupling, the coupling intensity or the number of particles determines how fast the synchronization state is reached.

When the criterion for the stationary regime Eq. (6) holds and the criterion for SR Eq. (14) fails [see the stationary regime without SR region of Fig. 3(a)], the first moment of the mean field is a monotonic function with respect to noise intensity [see the red solid line in Fig. 3(b)]. When both the criteria of the stationary regime Eq. (6) and SR Eq. (14) hold [see the stationary regime with SR region of Fig. 3(a)], the first moment of the mean field shows the SR phenomenon, which displays a nonmonotonic response with respect to noise intensity [see the blue solid line in Fig. 3(b)]. In Fig. 3(b), as the correlation parameter v increases, both the maximum value of the first moment and the corresponding noise intensity increase. In addition, in the stationary regime, the amplitude of the first moment of the mean field can be estimated reliably [see Fig. 3(b)]. Figure 3(b) shows that the proper intensity can lead to the maximum value of the first moment. When the criterion for the stationary regime Eq. (6) fails [see the nonstationary regime of Fig. 3(a)], with or without the criterion for the emergence of SR holding, the first moment of the mean field cannot be estimated reliably [see Fig. 3(b)]. This implies that the SR phenomenon cannot be observed in real applications and numerical simulations. The numerical results in Fig. 3 agree with the analytical results and show the parameter-induced transition between the stationary regime and the nonstationary regime.

The SR phenomenon can be explained by the correlation time of the noise. When the noise takes a large negative value, the system shows an unstable feature, which induces an unstable amplification response. Conversely, a positive noise intensity leads to stable evolution, which induces a stable response. With a proper frequency of the periodic source, a suitable correlation time can lead to cooperatively random switching between unstable amplification and stable response. Therefore, a proper noise intensity leads to the maximum value of the first moment [see Fig. 3(b)]. When the criterion for the stationary regime holds, the fluctuation of the response cannot reach a very high level due to the limitation of the stable second moment [see Fig. 1(a)]; otherwise, the fluctuation of the response can reach a very large level due to the unstable second moment [see Fig. 1(c)]. In addition, the lack of stability of the second moment indicates that the first moment cannot be estimated by averaging over the realizations [see Fig. 3(b)]. In the white noise case ($v \to +\infty$), the criterion for SR Eq. (14) fails for any Ω, σ, and a. This result means that nonmonotonic features cannot be found in the first moment of the mean field, which reflects the fact that the SR phenomenon strongly depends on the correlation time.

IV. DISCUSSION AND CONCLUSION

We started with a globally coupled Langevin system driven by a periodic force in a randomly switching potential. Subsequently, we introduced the moments of the mean field and the single particle displacements to profile the collective behavior of the stochastic system. Using a moment-based method, we show a convenient way to profile the collective behavior using the moments. After obtaining the steady-state solutions for the first moment and the criterion for the stationary regime, we analyzed the collective behavior of the complex system.

Based on the analytical results and numerical simulations, the importance of the stationary regime is stressed. The stationary regime can lead to the estimation-friendly data that can produce a more reliably estimated value for the first moment, especially for the small-sample experiment cases. Based on the criterion for the emergence of SR, the correlation time plays a key role. Furthermore, if the criterion for the stationary regime holds, the first moment of the mean field can be reliably estimated even if one of the two potential states is unstable. The parameter-induced stability is very important for realistic SR applications. Using this feature, one can effectively and reliably control the emergence of SR and provide some interpretations of the experimental results in applications in the future. In addition, the criterion for the stationary regime does not depend on the coupling, and we can apply the stationary regime criterion to the corresponding uncoupled stochastic system, e.g., the system studied in Ref. [16].

For a large coupling intensity or number of particles, we find that whether or not in the stationary regime, all of the particles would move synchronously, which shows us an equivalent way to investigate all of the particles in the system by just analyzing the mean field when the synchronization criterion holds. Thus, based on the synchronization criterion, the results of previous investigations into uncoupled system, e.g., the system studied in Ref. [16], can be extended to the harmonically coupled case.

In the nonstationary regime, we observed the volatility clustering phenomenon in the numerical simulations, which implies that the distribution of the mean field has the heavy-tailed property. This result indicates a potential mechanism for the generation of the heavy-tailed distribution and a connection between SR and heavy-tailed distributions.

The results of this work will supply valuable material for the corresponding experimental investigations and provide some possibilities for the interpretation of experimental cases. The results also suggest that coupled systems, which are important in real applications, will retain some interesting phenomena due to the interactions among the elements. A follow-up study will analyze the heterogeneous coupled fractional Langevin system in the sense of the stationary regime. We will also continue to investigate the connection between SR and volatility clustering.

ACKNOWLEDGMENTS

We would like to express our sincere appreciation and gratitude to the referee(s) and editors for their patience and constructive comments. We also thank Shu-Qiang Zhu for discussing the writing. The work was supported by the National Natural Science Foundation of China (Grant No. 11171238) and Natural Science Foundation for the Youth (Grant No. 11401405).

APPENDIX

Here, we provide some results for the following Langevin equation:

$$\frac{dz}{dt} + (a + \xi_t)z = A \sin \Omega t, \tag{A1}$$

where a, ξ_t, A, and Ω are the same as in the main text. By averaging over all realizations of the trajectory of the stochastic Eq. (A1), we obtain

$$\frac{d\langle z\rangle}{dt} + a\langle z\rangle + \langle \xi_t z\rangle = A \sin \Omega t. \tag{A2}$$

To find $\langle \xi_t z\rangle$, we multiply Eq. (A1) by ξ_t and average it. Then, we arrive at

$$\left\langle \xi_t \frac{dz}{dt} \right\rangle + a\langle \xi_t z\rangle + \sigma^2 \langle z\rangle = 0. \tag{A3}$$

Using the formulas of differentiation [29], also called the Shapiro-Loginov formulas, Eq. (A3) becomes

$$\frac{d\langle \xi_t z\rangle}{dt} + (a + 2v)\langle \xi_t z\rangle + \sigma^2 \langle z\rangle = 0. \tag{A4}$$

We denote $y_1 = \langle z\rangle$ and $y_2 = \langle \xi_t z\rangle$. Then, Eqs. (A2) and (A4) can be written as

$$\begin{aligned} \frac{dy_1}{dt} + ay_1 + y_2 &= A \sin \Omega t, \\ \frac{dy_2}{dt} + (a + 2v)y_2 + \sigma^2 y_1 &= 0. \end{aligned} \tag{A5}$$

To solve the closed Eqs. (A5), we use the Laplace transform and obtain

$$\begin{aligned} c_{11}Y_1 + c_{12}Y_2 &= y_1(0) + f, \\ c_{21}Y_1 + c_{22}Y_2 &= y_2(0), \end{aligned} \tag{A6}$$

with

$$f(s) = \frac{A\Omega}{s^2 + \Omega^2},$$

where $y_i(0)$ is the initial condition, $Y_i(s) = \int_0^{+\infty} y_i(t)e^{-st}dt$ is the Laplace transformation of $y_i(t)$ and $c_{ij} = (\mathbf{C})_{ij}$, where $\mathbf{C}$ is

$$\begin{pmatrix} s + a & 1 \\ \sigma^2 & s + a + 2v \end{pmatrix}.$$

By some algebraic operations, the solution of Eqs. (A6) can be represented in the form

$$\begin{aligned} Y_1(s) &= H_{10}(s)f + H_{11}(s)y_1(0) + H_{12}(s)y_2(0), \\ Y_2(s) &= H_{20}(s)f + H_{21}(s)y_1(0) + H_{22}(s)y_2(0), \end{aligned}$$

with

$$\begin{aligned} H_{10}(s) &= \frac{c_{22}}{c_{11}c_{22} - c_{12}c_{21}}, & H_{20}(s) &= \frac{-c_{21}}{c_{11}c_{22} - c_{12}c_{21}}, \\ H_{12}(s) &= \frac{-c_{12}}{c_{11}c_{22} - c_{12}c_{21}}, & H_{11}(s) &= \frac{c_{22}}{c_{11}c_{22} - c_{12}c_{21}}, \\ H_{21}(s) &= \frac{-c_{21}}{c_{11}c_{22} - c_{12}c_{21}}, & H_{22}(s) &= \frac{c_{11}}{c_{11}c_{22} - c_{12}c_{21}}. \end{aligned}$$

Using the inverse Laplace transformation, the time-domain solution for Eqs. (A5) can be directly written as the following:

$$\begin{aligned} y_1(t) &= A\int_0^t h_{10}(t-\tau)\sin(\Omega\tau)d\tau + \sum_{i=1}^{2} h_{1i}y_i(0), \\ y_2(t) &= A\int_0^t h_{20}(t-\tau)\sin(\Omega\tau)d\tau + \sum_{i=1}^{2} h_{2i}y_i(0), \end{aligned} \tag{A7}$$

where $h_{ij}(t)$ is the inverse Laplace transformation of $H_{ij}(s)$, for $i = 1,2$ and $j = 0,1,2$.

To find the steady-state solutions, we start with the characteristic equation of the system Eq. (A6),

$$a^2 + 2av - \sigma^2 + 2(a + v)s + s^2.$$

Using the Routh-Hurwitz stability criterion [44], we obtain the stability condition

$$\sigma^2 < a^2 + 2av. \tag{A8}$$

From the theoretical viewpoint, considering the stability condition Eq. (A8), the influence of the initial values will vanish as $t \to +\infty$. Without loss of generality, we consider all initial conditions to be zero in Eqs. (A7). Then, we can write the steady-state solutions of Eqs. (A5) as

$$\begin{aligned} \langle z(t)\rangle_{\mathrm{E}} &= A\int_0^t h_{10}(t-\tau)\sin(\Omega\tau)d\tau, \\ \langle \xi_t z(t)\rangle_{\mathrm{E}} &= A\int_0^t h_{20}(t-\tau)\sin(\Omega\tau)d\tau. \end{aligned}$$

There is an alternative way to calculate the above convolution instead of using the inverse Laplace transformation. Because the inhomogeneous term of Eqs. (A5) is a unique sinusoid, the steady-state solutions differ from the sinusoid waveform only in amplitude and phase angle [44]. More precisely, we have

$$\begin{aligned} \langle z(t)\rangle_{\mathrm{E}} &= A|H_{10}(j\Omega)|\sin(\Omega t + \phi_1), \\ \langle \xi_t z(t)\rangle_{\mathrm{E}} &= A|H_{20}(j\Omega)|\sin(\Omega t + \phi_2), \end{aligned} \tag{A9}$$

with $\phi_i = \arg H_{i0}(\mathrm{j}\Omega)$ for $i = 1,2$, where $j = \sqrt{-1}$ and

$$\begin{aligned} |H_{10}(\mathrm{j}\Omega)| &= \sqrt{\frac{\alpha_{11}^2 + \alpha_{12}^2}{\beta_1^2 + \beta_2^2}}, \tan\phi_1 = \frac{\alpha_{12}\beta_1 - \alpha_{11}\beta_2}{\alpha_{11}\beta_1 + \alpha_{12}\beta_2}, \\ |H_{20}(\mathrm{j}\Omega)| &= \sqrt{\frac{\alpha_{21}^2 + \alpha_{22}^2}{\beta_1^2 + \beta_2^2}}, \tan\phi_2 = \frac{\alpha_{22}\beta_1 - \alpha_{21}\beta_2}{\alpha_{21}\beta_1 + \alpha_{22}\beta_2}, \end{aligned} \tag{A10}$$

with

$$\begin{aligned} &\alpha_{11} = a + 2v, \quad \alpha_{12} = \Omega, \quad \alpha_{21} = -\sigma^2, \quad \alpha_{22} = 0, \\ &\beta_1 = a^2 + 2av - \Omega^2 - \sigma^2, \quad \beta_2 = 2(a + v)\Omega. \end{aligned} \tag{A11}$$

Next, we will give the stability criterion of variance $\langle(z-\langle z\rangle)^2\rangle$ for Eq. (A1). Subtracting Eq. (A2) from Eq. (A1), denoting $\tilde{z}=z-\langle z\rangle$, we obtain

$$\frac{d\tilde{z}}{dt}+a\tilde{z}+\xi_t\tilde{z}+\langle z\rangle\xi_t-\langle\xi_t z\rangle=0. \tag{A12}$$

Multiplying Eq. (A12) by $2\tilde{z}$ and $2\xi_t\tilde{z}$, respectively, we arrive at

$$\frac{d\tilde{z}^2}{dt}+2a\tilde{z}^2+2\xi_t\tilde{z}^2+2\langle z\rangle\xi_t\tilde{z}-2\langle\xi_t z\rangle\tilde{z}=0,\quad \xi_t\frac{d\tilde{z}^2}{dt}+2a\xi_t\tilde{z}^2+2\sigma^2\tilde{z}^2+2\langle z\rangle\sigma^2\tilde{z}-2\langle\xi_t z\rangle\xi_t\tilde{z}=0. \tag{A13}$$

Applying the formulas of differentiation [29] to Eqs. (A13), we obtain

$$\frac{d\langle\tilde{z}^2\rangle}{dt}+2a\langle\tilde{z}^2\rangle+2\langle\xi_t\tilde{z}^2\rangle+2\langle z\rangle\langle\xi_t z\rangle=0,\quad \frac{d\langle\xi_t\tilde{z}^2\rangle}{dt}+2(a+v)\langle\xi_t\tilde{z}^2\rangle+2\sigma^2\langle\tilde{z}^2\rangle-2\langle\xi_t z\rangle^2=0. \tag{A14}$$

Here, we notice the fact that $\langle\tilde{z}\rangle=0$ and $\langle z\rangle=\langle\tilde{z}\rangle$. Assuming that criterion Eq. (A8) holds, in the long-time regime, the above Eqs. (A14) trend to

$$\frac{d\langle\tilde{z}^2\rangle}{dt}+2a\langle\tilde{z}^2\rangle+2\langle\xi_t\tilde{z}^2\rangle=-2\langle z\rangle_{\mathrm{E}}\langle\xi_t z\rangle_{\mathrm{E}},\quad \frac{d\langle\xi_t\tilde{z}^2\rangle}{dt}+2(a+v)\langle\xi_t\tilde{z}^2\rangle+2\sigma^2\langle\tilde{z}^2\rangle=2\langle\xi_t z\rangle_{\mathrm{E}}^2. \tag{A15}$$

Because the input items, i.e., the right-hand side of Eqs. (A15), are bounded, according to Eqs. (A9), the stability depends on the corresponding homogeneous part [44]. Applying the Routh-Hurwitz stability criterion [44], we obtain the stability condition

$$\sigma^2<a^2+av. \tag{A16}$$

[1] L. Gammaitoni, P. Hänggi, P. Jung, and F. Marchesoni, Rev. Mod. Phys. **70**, 223 (1998).
[2] H. Chen, P. K. Varshney, S. M. Kay, and J. H. Michels, IEEE Trans. Signal Process **55**, 3172 (2007).
[3] R. Benzi, A. Sutera, and A. Vulpiani, J. Phys. A **14**, L453 (1981).
[4] K. Wiesenfeld and F. Moss, Nature **373**, 33 (1995).
[5] P. Hänggi, Chem. Phys. Chem. **3**, 285 (2002).
[6] W. Zhang and B.-R. Xiang, Talanta **70**, 267 (2006).
[7] E. Soika, R. Mankin, and A. Ainsaar, Phys. Rev. E **81**, 011141 (2010).
[8] R. Mankin, K. Laas, T. Laas, and E. Reiter, Phys. Rev. E **78**, 031120 (2008).
[9] Hu Gang, T. Ditzinger, C. Z. Ning, and H. Haken, Phys. Rev. Lett. **71**, 807 (1993).
[10] C. J. Tessone, C. R. Mirasso, R. Toral, and J. D. Gunton, Phys. Rev. Lett. **97**, 194101 (2006).
[11] Y. Atsumi, S. Hata, and H. Nakao, Phys. Rev. E **88**, 052806 (2013).
[12] Y. Tang, W. Zou, J. Lu, and J. Kurths, Phys. Rev. E **85**, 046207 (2012).
[13] A. Pikovsky, A. Zaikin, and M. A. de la Casa, Phys. Rev. Lett. **88**, 050601 (2002).
[14] D. Cubero, Phys. Rev. E **77**, 021112 (2008).
[15] M. Gitterman, Physica A **352**, 309 (2005).
[16] S. Jiang, F. Guo, Y. Zhou, and T. Gu, Physica A **375**, 483 (2007).
[17] G.-T. He, Y. Tian, and Y. Wang, J. Stat. Mech. (2013) P09026.
[18] G.-T. He, Y. Tian, and M.-K. Luo, J. Stat. Mech. (2014) P05018.
[19] G.-T. He, R.-Z. Luo, and M.-K. Luo, Phys. Scr. **88**, 065009 (2013).
[20] S. Zhong, H. Ma, H. Peng, and L. Zhang, Nonlinear Dyn. **82**, 535 (2015).
[21] T. Yu, L. Zhang, and M.-K. Luo, Phys. Scr. **88**, 045008 (2013).
[22] J.-H. Li and Y.-X. Han, Phys. Rev. E **74**, 051115 (2006).
[23] J.-H. Li, Phys. Rev. E **66**, 031104 (2002).
[24] J.-H. Li and Y.-X. Han, Commun. Theor. Phys. **47**, 672 (2007).
[25] J.-H. Li, Chaos **21**, 043115 (2011).
[26] L. S. Tsimring, Rep. Prog. Phys. **77**, 026601 (2014).
[27] F. Droste and B. Lindner, Biol. Cybern. **108**, 825 (2014).
[28] C. Van Den Broeck, J. Stat. Phys. **31**, 467 (1983).
[29] V. E. Shapiro and V. M. Loginov, Physica A **91**, 563 (1978).
[30] P. Reimann and T. C. Elston, Phys. Rev. Lett. **77**, 5328 (1996).
[31] M. Si, N. Conrad, S. Shin, J. Gu, J. Zhang, M. Alam, and P. Ye, IEEE Trans. Electron Devices **62**, 3508 (2015).
[32] S. Boccaletti, V. Latora, Y. Moreno, M. Chavez, and D.-U. Hwang, Phys. Rep. **424**, 175 (2006).
[33] R. C. Bourret, U. Frisch, and A. Pouquet, Physica **65**, 303 (1973).
[34] R. C. Desai and R. Zwanzig, J. Stat. Phys. **19**, 1 (1978).
[35] R. Mankin, K. Laas, and N. Lumi, Phys. Rev. E **88**, 042142 (2013).
[36] B. Mandelbrot, J. Bus. **36**, 394 (1963).
[37] R. D. Astumian and M. Bier, Phys. Rev. Lett. **72**, 1766 (1994).
[38] J. H. Li and Z. Q. Huang, Phys. Rev. E **57**, 3917 (1998).
[39] M. Bier, Contemp. Phys. **38**, 371 (1997).
[40] E. B. Stukalin, H. Phillips, and A. B. Kolomeisky, Phys. Rev. Lett. **94**, 238101 (2005).
[41] J.-P. Lv, H. Liu, and Q.-H. Chen, Phys. Rev. B **79**, 104512 (2009).
[42] A. G. Hendricks, B. I. Epureanu, and E. Meyhöfer, Phys. Rev. E **79**, 031929 (2009).
[43] C. Kim, E. K. Lee, and P. Talkner, Phys. Rev. E **73**, 026101 (2006).
[44] R. C. Dorf and R. H. Bishop, *Modern Control Systems*, 12th ed. (Pearson, Prentice Hall, 2010).